Short Pigment Epithelial-Derived Factor-Derived Peptide Inhibits Angiogenesis and Tumor Growth

Yelena Mirochnik,[1] Arin Aurora,[1,4] Frank T. Schulze-Hoepfner,[1,3] Ahmed Deabes,[1] Victor Shifrin,[5] Richard Beckmann,[2] Charles Polsky,[2] and Olga V. Volpert[1]

Abstract

Purpose: Pigment epithelial-derived factor (PEDF) is a potent angiogenesis inhibitor with multiple other functions, some of which enhance tumor growth. Our previous studies mapped PEDF antiangiogenic and prosurvival activities to distinct epitopes. This study was aimed to determine the minimal fragment of PEDF, which maintains antiangiogenic and antitumor efficacy.

Experimental Design: We analyzed antigenicity, hydrophilicity, and charge distribution of the angioinhibitory epitope (the 34-mer) and designed three peptides covering its COOH terminus, P14, P18, and P23. We analyzed their ability to block endothelial cell chemotaxis and induce apoptosis *in vitro* and their antiangiogenic activity *in vivo*. The selected peptide was tested for the antitumor activity against mildly aggressive xenografted prostate carcinoma and highly aggressive renal cell carcinoma. To verify that P18 acts in the same manner as PEDF, we used immunohistochemistry to measure PEDF targets, vascular endothelial growth factor receptor 2, and CD95 ligand expression in P18-treated vasculature.

Results: P14 and P18 blocked endothelial cell chemotaxis; P18 and P23 induced apoptosis. P18 showed the highest IC_{50} and blocked angiogenesis *in vivo*: P23 was inactive and P14 was proangiogenic. P18 increased the production of CD95 ligand and reduced the expression of vascular endothelial growth factor receptor 2 by the endothelial cells *in vivo*. In tumor studies, P18 was more effective in blocking the angiogenesis and growth of the prostate cancer than parental 34-mer; in the renal cell carcinoma, P18 strongly decreased angiogenesis and halted the progression of established tumors.

Conclusions: P18 is a novel and potent antiangiogenic biotherapeutic agent that has potential to be developed for the treatment of prostate and renal cancer.

Angiogenesis (the formation of new capillaries from established ones) is a necessary prerequisite for the exponential tumor growth. Angiogenesis is regulated by the balance between positive and negative regulators, inhibitors and stimuli, in the tumor microenvironment also termed angiogenic switch: in the normal tissue, the prevalence of inhibitors maintains vascular quiescence, whereas, in tumors, the balance is tipped in favor of the stimuli (1). Angiogenic switch can be flipped back to the "off position" by sequestering angiogenic stimuli with appropriate neutralizing antibodies, by blocking their signaling receptors using small-molecule inhibitors, or by employing natural antiangiogenic molecules. The advent of therapies targeting proangiogenic vascular endothelial growth factor (VEGF) and platelet-derived growth factor-BB or their receptors (Avastin, sunitinib, and sorafenib; refs. 2, 3) underscores the therapeutic value of antiangiogenics but also highlights the possibility of overcoming the withdrawal of a single angiogenic factor (4). Studies of past two decades suggest that natural inhibitors of angiogenesis act as endothelial-specific tumor suppressors (5); their specificity for remodeling endothelium and the interference with multiple proangiogenic factors make natural inhibitors and their derivatives an attractive alternative to the blockade of the individual angiogenic stimuli (6, 7).

Pigment epithelial-derived factor (PEDF) is a potent and versatile angiogenesis inhibitor (8): it is active against wide range of angiogenic stimuli, including VEGF, basic fibroblast growth factor (bFGF), platelet-derived growth factor-BB, and interleukin-8 (8). The loss of PEDF is common for multiple human cancers: recent studies indicate the link among decreased PEDF expression, higher microvascular density (MVD), and aggressive, metastatic phenotype in the carcinomas of prostate and pancreas, gliomas, and non-small cell lung cancer (reviewed in ref. 9). PEDF overexpression in melanoma, prostate and ovarian carcinoma, pancreatic cancer, osteosarcoma, Wilm's tumor, and neuroblastoma cell lines causes

Authors' Affiliations: [1]Urology Department, Northwestern University Feinberg School of Medicine; [2]Arbus Pharmaceuticals, Chicago, Illinois; [3]Department of Urology, Johann Wolfgang Goethe-Universitaet, Frankfurt, Germany; [4]Department of Molecular Biology, University of Texas Southwestern Medical Center, Dallas, Texas; and [5]International Consulting, Inc., Auburndale, Massachusetts

Received 8/11/08; revised 10/21/08; accepted 10/21/08; published OnlineFirst 02/17/2009.

Grant support: NIH grants RO1 HL068033 and RO1 HL077471 (O.V. Volpert), Department of Defense Prostate Cancer Research Program of the Congressionally Directed Medical Research Programs fellowship W81XWH-06-1-0103 (Y. Mirochnik), and Arbus Pharmaceuticals (R. Beckmann, C. Polsky, O.V. Volpert, and V. Shifrin).

The costs of publication of this article were defrayed in part by the payment of page charges. This article must therefore be hereby marked *advertisement* in accordance with 18 U.S.C. Section 1734 solely to indicate this fact.

Requests for reprints: Olga V. Volpert, Department of Urology Northwestern University Feinberg School of Medicine, Chicago, IL 60611. Phone: 312-503-5934; Fax: 312-908-7275; E-mail: olgavolp@northwestern.edu.

doi:10.1158/1078-0432.CCR-08-2113

Translational Relevance

Angiogenesis is requisite for the exponential tumor growth: antiangiogenic therapies, such as Avastin, have emerged as important new modalities for cancer treatment. Pigment epithelial-derived factor (PEDF) is a potent naturally occurring inhibitor of angiogenesis: PEDF reexpression in multiple tumor types including melanoma, prostate cancer, and ovarian cancer delays the onset of primary tumors and decreases metastases. However, clinical use of the native PEDF would be costly and complicated due to its multiple biological activities and antigenicity. We previously identified PEDF antiangiogenic epitopes. Here, we designed peptides covering its most potent antiangiogenic region, the 34-mer. Using series of the *in vivo* and *in vitro* angiogenesis assays, we screened these peptides and selected one, P18, which showed efficacy against relatively mild prostate cancer and highly aggressive renal cell carcinoma. P18 is a short peptide with specific activity in a low nanomolar range and a candidate biological drug for clinical testing.

dramatic reductions in MVD, tumor burden, and metastases (9, 10), suggesting PEDF as a promising therapeutic target. In addition to its antiangiogenic activity, PEDF acts as survival factor for the neural crest cells; it also stimulates expansion of the stem cell niche in the brain and induces differentiation toward neuronal phenotype in multiple cell types (11, 12).

We have previously mapped PEDF antiangiogenic function to the NH_2-terminal surface epitope (the 34-mer amino acid residues 24-57; ref. 13). PEDF prosurvival and neurodifferentiating functions have been mapped to the adjacent epitope (44-mer residues 58-101; refs. 10, 14, 15). Combined with the results of binding studies, data by us and others indicate that PEDF can bind two nonidentical receptors that trigger distinct signaling cascades, leading to different functional outcomes (13). Recently, one PEDF receptor, a phospholypase A2, has been identified, which is likely to transmit PEDF prosurvival and differentiating signals (16); the antiangiogenic PEDF receptor remains elusive.

Although overexpression of the native PEDF is effective in delaying growth, treatment with native protein is less feasible due to antigenicity and stability issues as well as prohibitive production costs. In addition, prosurvival function of exogenously added PEDF may oppose its antitumor effect; indeed, both PEDF at high concentrations and 44-mer are proangiogenic (13, 17), suggesting the existence of the second, low-affinity endothelial receptor for the 44-mer epitope. Neuroendocrine differentiation of cancer cells due to the 44-mer may also augment tumor growth and angiogenesis, because neuroendocrine cells secrete high levels of growth factors and cytokines, which are also proangiogenic (18). Thus, using PEDF derivatives, which retain only antiangiogenic activity, could be more practical. Small peptides (<20 amino acids) are usually less likely to generate immune response; they are also more effectively absorbed through the oral mucosa by passive diffusion (19). Although small peptides might have short half-life *in vivo*, that obstacle can be overcome by chemical modifications.

In the study below, we identified minimal active peptide within the antiangiogenic 34-mer epitope (P18). P18 *in vitro* activity was similar to that of the 34-mer. *In vivo*, however, P18 inhibited angiogenesis and the growth of moderately aggressive prostate cancer and of highly aggressive renal cell carcinoma (RCC), whereas the 34-mer produced no significant effect. P18 altered the expression of the two PEDF signaling targets critical for its antiangiogenic action, VEGF receptor (VEGFR; ref. 20) and CD95 ligand (CD95L; ref. 13), in P18-treated animals: the proportion of the VEGFR-positive microvessels was decreased in response to P18, whereas the percentage of vascular structures positive for CD95L became significantly higher, suggesting that P18 shares molecular targets and signaling cascades with parental PEDF.

Materials and Methods

Cells and reagents. Human umbilical vein and microvascular endothelial cells (Lonza) were maintained at 5% CO_2 in MCDB131 medium (Sigma) supplemented with endothelial cell bullet kit, 5% fetal bovine serum (Lonza), and 1% penicillin-streptomycin mix; the cells were used at passages 6 to 9. Prostate carcinoma cells PC-3 (American Tissue Type Culture Collection) were maintained at 5% CO_2 in RPMI (Mediatech), 10% fetal bovine serum, and 1% penicillin-streptomycin mix. Renca cells (a gift from Dr. Chung Lee, Northwestern University Urology Department) were maintained at 5% CO_2 in DMEM (Mediatech) and 10% fetal bovine serum.

VEGF and bFGF were purchased from R&D Systems and Matrigel was purchased from BD Biosciences.

Three nested peptides covering the COOH terminus of PEDF antiangiogenic epitope (the 34-mer ref. 13) were synthesized to order at GenScript (>95% purity) and characterized by mass spectrometry: P14 (residues 43-57 of PEDF molecule), P18 (residues 39-57), and P23 (residues 34-57). The peptides were acetylated at the NH_2 termini and amidated at the COOH termini for stability. Stock solutions (6 mmol/L) were made in DMSO and stored at -20°C. Working dilutions were made in maintenance medium or in PBS and used immediately.

Endothelial cell chemotaxis assay was done as described previously (21): briefly, endothelial cells were starved overnight in serum-free medium supplemented with 0.1% bovine serum albumin (Sigma), harvested, suspended at 1.5×10^6/mL, plated on the lower side of gelatinized microporous membranes (8 μm pores, Nuclepore; Whatman) in the inverted modified Boyden chambers (Applied Biosystems), and allowed 2 h to adhere at culture conditions (37°C, 5% CO_2). The test substances were diluted in MCDB131, 0.1% bovine serum albumin and added to the upper wells of the chamber, the cells incubated for additional 3 to 4 h. The membranes were then recovered fixed, stained and mounted on slides. Migrated cells in each well were counted in 10 random high power (400×) fields. Each sample was tested in quadruplicate for statistical evaluation. bFGF (20 ng/mL), used to induce chemotaxis, served as a positive control, MCDB131 with 0.1% bovine serum albumin was considered a negative control (random, nondirectional migration).

Viability assay. Tumor cells were seeded at 1×10^3 per well in the 96-well tissue culture plate and treated with increasing peptide concentrations from 100 pmol/L to 1 μmol/L. After 48 h, the number of viable cells was assessed using MTT assay kit (Biotium) according to the manufacturer's instructions.

Endothelial cell apoptosis was measured using terminal deoxynucleotidyl transferase-mediated dUTP nick end labeling (TUNEL) assay kit (Chemicon) as recommended by manufacturer. Confluent human microvascular endothelial cells grown on coverslips were treated overnight with PEDF or PEDF peptides with or without protective bFGF (20 ng/mL) in MCDB131 supplemented with low serum (0.2% fetal bovine serum). The cells were counterstained with propidium iodide; three to five ×10 fields were analyzed using epifluorescent microscope: total cell number (propidium iodide-positive cells) and

TUNEL-positive cells were quantified using MetaMorph software (Molecular Devices) and % apoptotic cells were calculated.

Animals. Six- to 8-week-old female athymic nude mice (*nu/nu*) or C57/BLJ6 mice (Harlan) were kept in pathogen-free environment; autoclaved water and γ-irradiated commercial diet were provided *ad libitum*. All manipulations were done under sterile conditions according to the institutional guidelines and in compliance with the Guide for Care and Use of Laboratory Animals (NIH).

Mouse corneal angiogenesis assay was done as described previously (22): briefly, the peptides were incorporated in slow-release hydron-sucralfate pellets (~1 μL) containing bFGF (250 ng/mL). The pellets were implanted in the cornea of C57/BL6J mice. bFGF served as positive control. Angiogenesis was monitored by slit-lamp microscopy and the pictures were taken on days 5 to 7 post-implantation. Ingrowth of the blood vessels into avascular cornea toward pellets was scored as positive response. The results are reported as positive corneas of total implanted.

Directed* in vivo *angiogenesis assay. Small cylindrical silicon angioreactors were filled with basement membrane extract containing proangiogenic factors (bFGF/VEGF mix) and the peptides (1 μmol/L) were implanted subcutaneously in both flanks of nude mice (two reactors per side, four reactors per animal). After 12 days, the reactors were excised and the contents were processed as recommended by the manufacturer. The cells were labeled with FITC-lectin and fluorescence was measured. Fluorescence intensity reflects the number of endothelial cells that entered the angioreactors and is a quantitative measure of angiogenic response. All reagents for the assay were provided in Directed *In vivo* Angiogenesis Assay (DIVAA) Inhibition kit (Trevigen).

Matrigel plug assay was done as described elsewhere (23). Matrigel (BD Biosciences) was mixed with bFGF (250 ng/mL) with or without PEDF peptides (1 or 10 nmol/L, as indicated) and injected subcutaneously in the median abdominal area of nude mice. After 10 days, the plugs were excised, snap frozen in liquid nitrogen, and sectioned to a 5 μm thickness.

Immunohistochemistry. Frozen sections were fixed in sequential changes of acetone/acetone and chloroform/acetone at -20°C; the sections were stained with anti-CD31 rat anti-mouse antibody (4μg/mL; BD Biosciences) followed by the donkey anti-rat rhodamine red-X conjugate (1:200 dilution; Jackson ImmunoResearch Labs) to detect blood vessels. Rabbit anti-mouse human CD95 or CD95L antibodies (Calbiochem) were used at 2.5 μg/mL and visualized using donkey anti-rabbit secondary antibodies conjugated with Cy5 (1:100; Jackson ImmunoResearch). To detect VEGFR2, we used rabbit anti-mouse antibodies (Santa Cruz Biotechnology) and donkey anti-rabbit Cy2-conjugated secondary antibodies (Jackson ImmunoResearch). *In situ* TUNEL assay was done using Apoptag staining kit (Chemicon International) according to the manufacturer's instructions.

Tumorigenicity assay. Hormone-refractory human prostate cancer cells PC-3 were implanted by subcutaneous injections in the right flank region of female nude mice (2×10^6 per site). The treatment was commenced after the tumors became palpable and measurable. Highly aggressive mouse renal carcinoma cells (Renca) were implanted in the same manner (1×10^6 per site) and allowed to reach 100 to 200 mm^3. Vehicle PBS or PEDF peptides (P18 and the 34-mer, 10 mg/kg) were administered by intraperitoneal injections every 2 days. Tumor progression was monitored 25 days for the PC-3 cells and 10 days for Renca cells; tumors were measured every 2 to 3 days and the volumes were calculated as length × width^2 × 0.523 (24). Renca tumors were also excised and weighted at the completion of experiment.

Statistical analysis. All numerical data were analyzed with GraphPad Prism 5.0 (GraphPad Software) using Student's *t* test, one-way ANOVA, or repeated-measures ANOVA where appropriate. *P* values < 0.05 were considered statistically significant.

Results

***Short derivatives of the PEDF 34-mer epitope block endothelial cell chemotaxis and survival* in vitro.** The angioinhibitory activity of PEDF was mapped to the highly conserved 34-mer surface epitope (13). We analyzed the three-dimensional structure of the 34-mer fragment using Protean software (Lasergene, DNA Star package; DNA Star) for the hydrophobic regions and charge distribution (Fig. 1A). The hydrophilic COOH terminus with highly charged central area had the highest

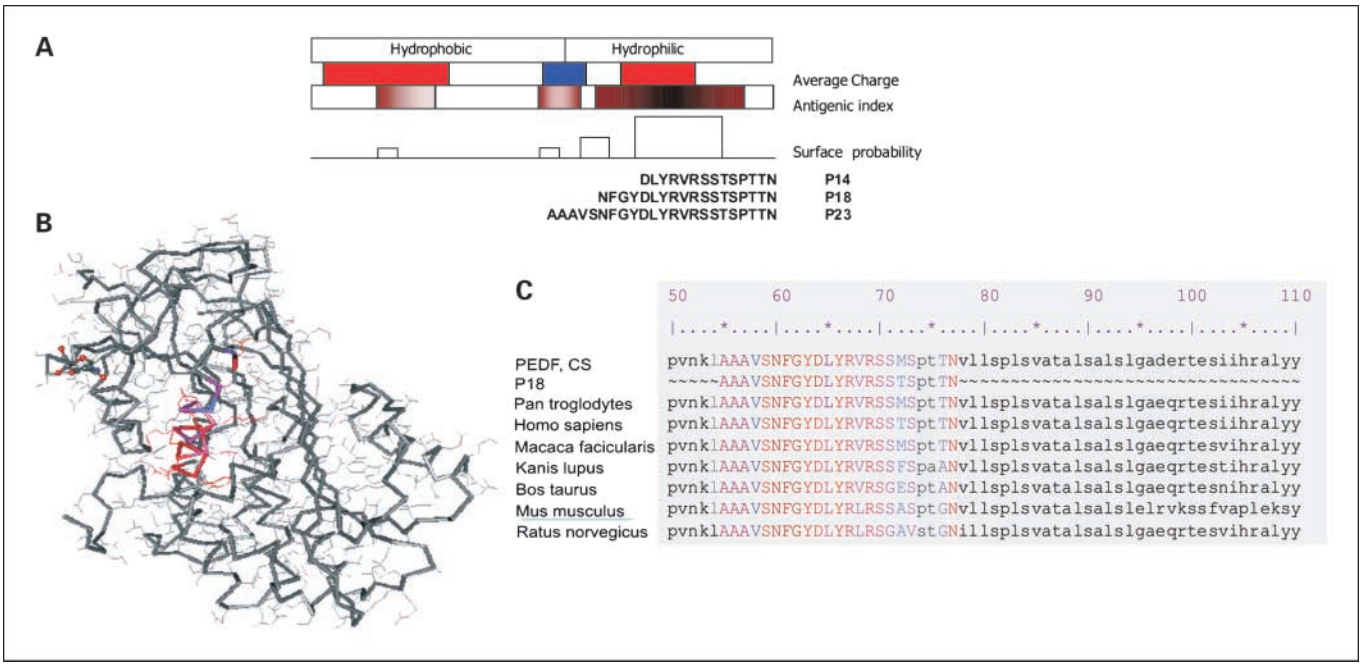

Fig. 1. Design of the short peptide derivatives of PEDF 34-mer epitope. *A,* Protean analysis of the 34-mer sequence for surface presentation, hydrophilicity profile, and antigenic index. Three nested peptides covering hydrophilic stretch of the 34-mer. *B,* crystal structure of the PEDF molecule: 23-amino acid hydrophilic part of the 34-mer surface epitope is highlighted (generated using Cn3D4.1 software). *Red,* positive charged stretches; *blue,* negatively charged stretches. *C,* alignment of the 23-amino acid hydrophilic stretch with available PEDF sequences (GenBank) shows high conservation among the species.

potential for the intramolecular interactions, including the target receptor. We designed three short overlapping peptides covering the 34-mer COOH terminus termed according to their length P14 (amino acids 43-57 of the PEDF molecule), P18 (residues 39-57), and P23 (residues 34-57; Fig. 1A). All the 23 amino acids are at the surface of the molecule and likely to interact with the putative angiogenic receptor (Fig. 1B); high degree of homology between species (Fig. 1C) in this part of the PEDF molecule also suggests its functional importance.

As an indicator of antiangiogenic activity, we measured the ability of the peptides to inhibit endothelial cell chemotaxis along the gradient of angiogenic stimulus (25). Dose-response analysis (Fig. 2A) has yielded IC_{50} of 10 and 1 pmol/L for the P14 and P18, respectively. The P23 had no inhibitory effect. As shown previously (8, 13), PEDF and the 34-mer have IC_{50} of 400 and 100 pmol/L, respectively. P14 was slightly cytotoxic in a 4-h assay at concentrations above 10 nmol/L; P18 and P23 showed no cytotoxic activity (data not shown).

PEDF and the 34-mer block angiogenesis by inducing endothelial cell apoptosis (13, 26). We therefore compared the apoptotic effects of P14, P18, and P23 with that of the parental 34-mer. In human microvascular endothelial cells, overnight serum deprivation (0.2% fetal bovine serum) causes significant levels of apoptosis, which was relieved by protective bFGF (Fig. 2C). In low serum, the 34-mer and P23 enhanced stress-induced apoptosis, whereas PEDF and P18 had no effect

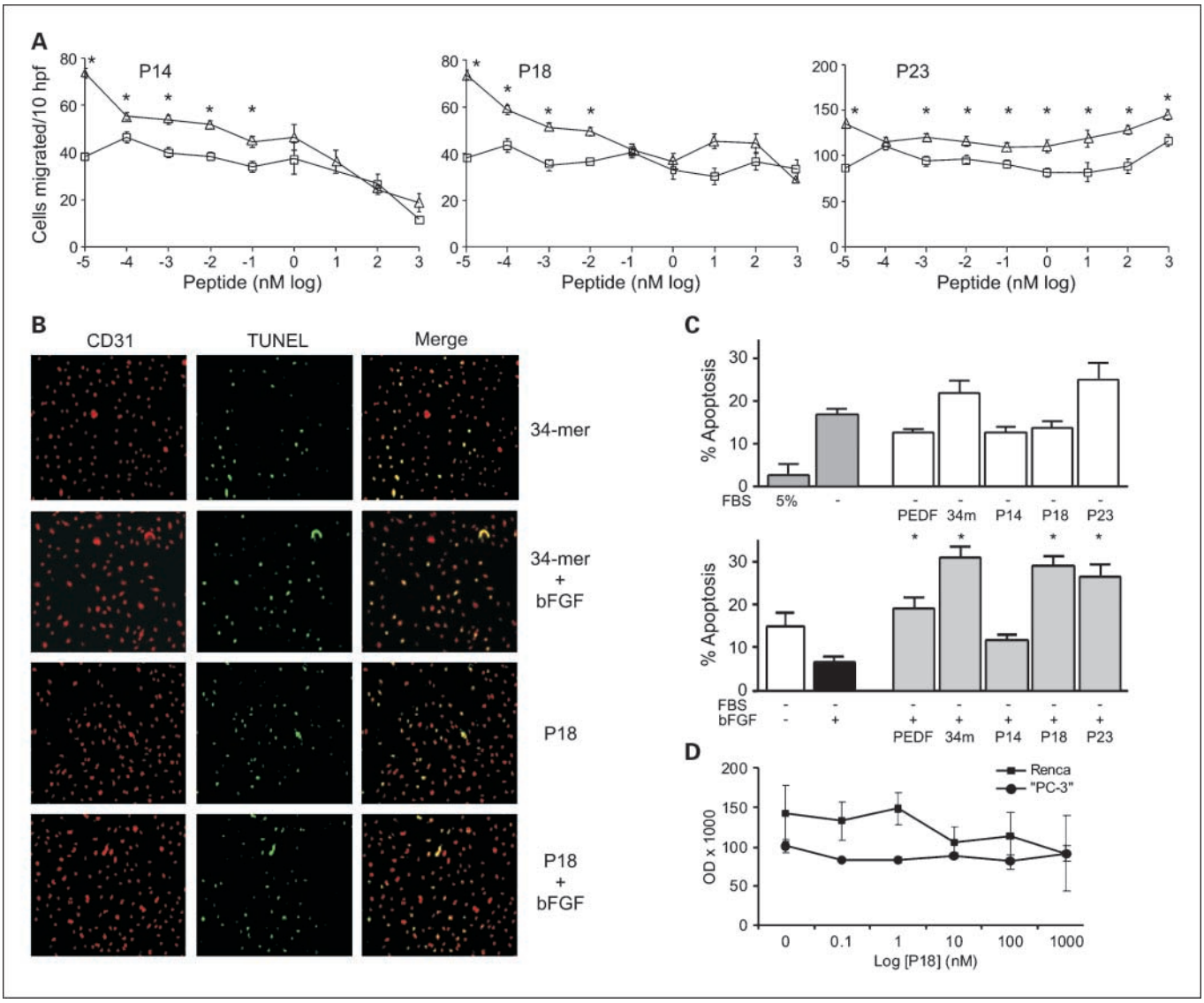

Fig. 2. *In vitro* screening of the short peptide derivatives of PEDF 34-mer epitope. *A,* representative endothelial cell (human umbilical vein endothelial cells) chemotaxis assays: P14, P18, and P23 were tested at increasing concentrations alone (□) or in combination with bFGF (△). The assay was done independently for each peptide; each peptide concentration was tested in quadruplicate to achieve statistical significance and the experiment was repeated three times. *, $P < 0.001$, significantly different from the background control (bovine serum albumin alone). Note the inhibition of bFGF-induced chemotaxis by P14 and P18 but not P23. *hpf,* high-powered fields. *B* and *D,* induction of human microvascular endothelial cell apoptosis by PEDF peptides: the cells were plated on coverslips and incubated overnight with P14, P18, and P23 in low-serum medium alone or in the presence of protective bFGF. Apoptosis was detected by TUNEL. PEDF (10 nmol/L) and the 34-mer (100 nmol/L) were used as control. Representative images (*B*). *C,* neither of the peptides significantly augmented apoptosis by serum withdrawal ($P = 0.06$; *top*). However, P18 and P23 overcame the protective effect of bFGF ($P < 0.008$; *bottom*). *, $P < 0.05$. Note the lack of apoptosis in the presence of P14. Mean ± SD. *D,* P18 had no effect on tumor cells. PC-3 and Renca cells were treated with increasing concentrations of P18 and the numbers of viable cells were evaluated by MTT assay. Note the lack of significant differences in cell numbers with increasing P18 concentration.

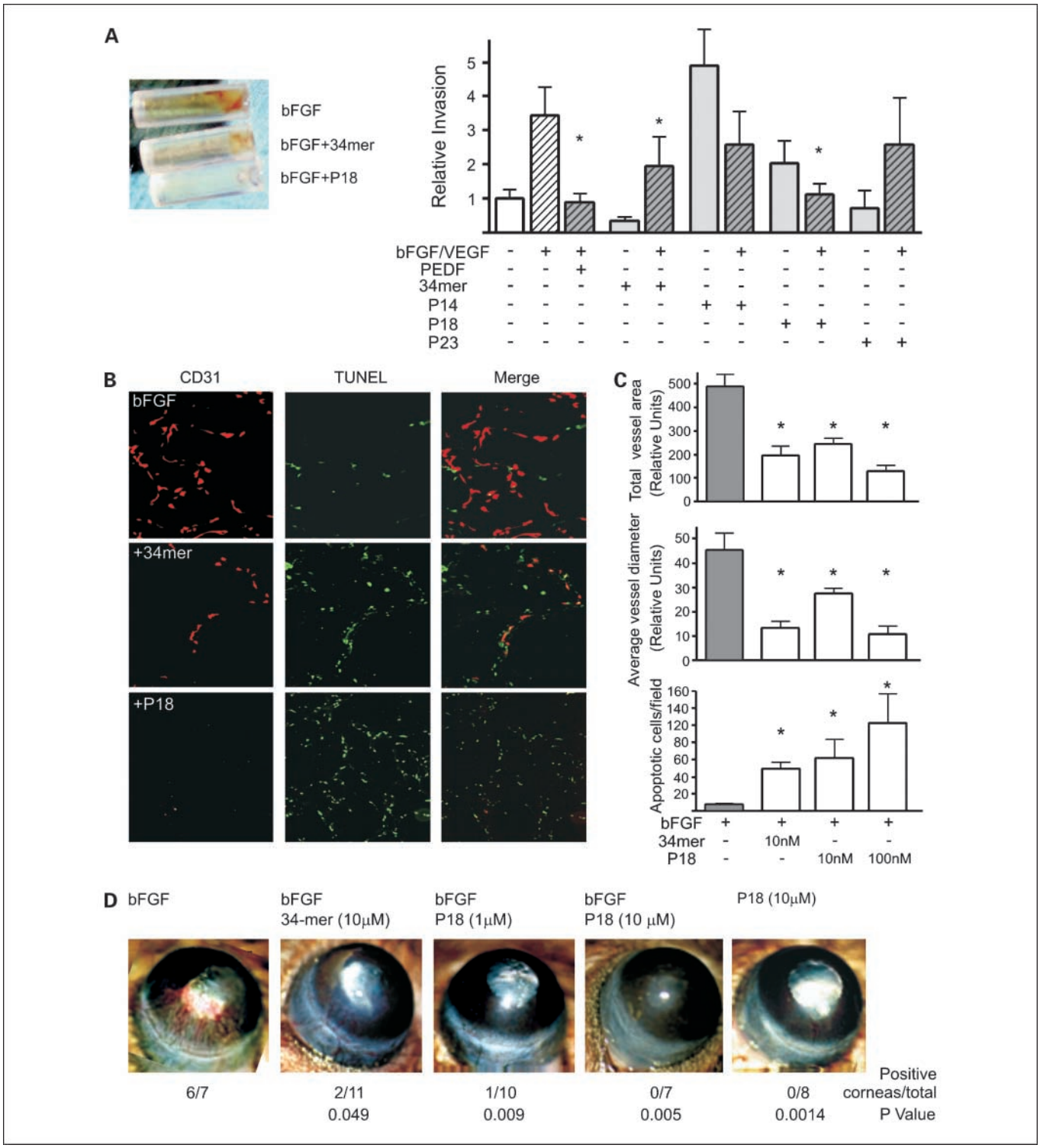

Fig. 3. *In vivo* testing of the antiangiogenic properties of PEDF short peptides. *A,* DIVAA: the invasion of the vasculature into open-ended angioreactors filled with the basement matrix (*left*) is measured by lectin staining of the endothelial cells liberated from the reactors at the completion of experiment (10 d). Three independent experiments were done and normalized per negative control; average fluorescence values were calculated. Angiogenic activity was expressed as relative invasion of the endothelial cells (*right*). The peptides were tested at 10 nmol/L alone (*gray columns*) or in the presence of bFGF/VEGF mix (*hatched columns*). PEDF (20 nmol/L) and the 34-mer (100 nmol/L) were used as controls. Note the induction of angiogenesis by P14 and lack of inhibitory activity by P23. *Asterisks,* significantly lower than bFGF-induced invasion. *B* and *C,* P18 was tested at 1 and 10 nmol/L in the conventional 11-day Matrigel assay with and without bFGF (100 ng/mL). Ten Matrigel plugs were tested per condition. *B,* at the time of harvest, Matrigel plugs were snap-frozen, sectioned, and stained for the endothelial marker CD31 (*red*). Apoptosis was detected by *in situ* TUNEL (*green*). Merged images are shown to visualize apoptotic endothelial cells. The 34-mer (10 nmol/L) was used to control for the inhibitory activity. *C,* vascularization [total vessel area (*top*) and average vessel diameter (*middle*)] and apoptosis (*bottom*) were quantified by MetaMorph software (Molecular Devices). *, $P < 0.01$, significantly different from bFGF. Statistical significance was calculated by one-way ANOVA and Dunnett's multiple comparison test. *D,* P18 angioinhibitory activity was verified in the mouse cornea assay for angiogenesis. The 34-mer was used to control for the inhibitory activity. Representative cornea, final scoring (positive cornea of total implanted), and statistical significance. Statistical significance was calculated by Fisher's exact test.

(Fig. 2C). As expected, in the presence of protective bFGF, the 34-mer was proapoptotic and P18 and P23 caused apoptosis in the bFGF-induced endothelial cells (Fig. 2C). P14 failed to induce endothelial cell apoptosis (Fig. 2C), although it was effective in migration assay (Fig. 2B). The effect of the P18 was restricted to the endothelial cells: the survival rates of PC-3 and Renca cells were not significantly inhibited by P18 at concentrations up to 1 μmol/L (Fig. 2D).

***P18 blocked angiogenesis and induced endothelial cell apoptosis* in vivo.** Based on their antiangiogenic function *in vitro*, we tested P18, P14, and P23 in the three *in vivo* assays for angiogenesis: corneal micropocket assay, DIVAA, and Matrigel plug assay. In a more quantitative DIVAA assay (Fig. 3A), bFGF/VEGF increased angiogenesis ~3-fold over negative control (basement membrane extract; $P = 0.01$). PEDF, 34-mer, and P18 blocked bFGF/VEGF action. PEDF and P18 were the most effective reducing level of vascularization to the level of basement membrane extract ($P = 0.006$ and 0.01, respectively). P18 showed stronger inhibitory effect than the 34-mer. P14 and P23 had little effect on angiogenic response elicited by the FGF/VEGF combination (Fig. 3A); however, P14 alone was proangiogenic ($P < 0.05$). Matrigel plug assay is similar to the DIVAA but performed on a larger scale: it provides an opportunity to section the plugs and evaluate the morphology of the neovessels and endothelial cell apoptosis in addition to the MVD (Fig. 3B and C). As in DIVAA, both 34-mer and P18 at 10 nmol/L caused a 3-fold decrease in MVD measured as total $CD31^+$ area ($P < 0.001$; Fig. 3C, *top*). We also evaluated mean diameter of the neovessels and detected ~4-fold decrease ($P < 0.01$; Fig. 3C, *middle*). The response to P18 was clearly dose-dependent. Moreover, whereas both 34-mer and P18 induced significant levels of endothelial cell apoptosis as measured by *in situ* TUNEL, the apoptotic effect of P18 was significantly more robust at 100 nmol/L ($P < 0.01$; Fig. 3C, *bottom*). In the cornea assay, P18 was able to block bFGF-induced angiogenesis to the extent similar to the 34-mer (Fig. 3D).

P18 inhibits the growth and angiogenesis of prostate and renal cancer xenografts. The exponential growth of solid tumors is contingent on angiogenesis. We therefore tested the effect of the P18 on tumor growth and angiogenesis. Androgen-independent human prostate cancer cells PC-3 were injected subcutaneously into the flanks of nude mice. When palpable tumors were established, the animals were treated with the 34-mer, P18, or control vehicle. P18 administered every 2 days at 10 mg/kg strongly inhibited the growth of PC-3 xenografts, whereas the 34-mer had no significant effect (Fig. 4A). The differences were statistically significant ($P < 0.001$) as was calculated by repeated-measures ANOVA. P18 also halted the growth of highly aggressive RCC: P18 treatment of mice bearing established 150- to 200-mm^3 tumors formed by mouse Renca RCC cells caused ~4-fold reduction in tumor volume and weight after 10 days of treatment compared with the vehicle control ($P < 0.004$ and $P < 0.0002$, respectively; Fig. 4B and C). An ~3-fold decrease in tumor volume in P18-treated animals bearing PC-3 tumors ($P < 0.001$; Fig. 4A) was accompanied by a dramatic decrease in angiogenesis (Fig. 5A and B): total vascular area and average vessel diameter were reduced by 2.7-fold ($P < 0.05$; Fig. 5B, *top*) and 4.8-fold ($P < 0.001$; Fig. 5B, *middle*), respectively. Decreased vascularization was paralleled by ~3-fold increase ($P < 0.001$) in the apoptotic cells, both endothelial cells and tumor cells proper (Fig. 5B, *bottom*). We observed similar reduction in vascularization of the more aggressive RCC tumor grafts (Fig. 5C and D); the decreased cellularity of the P18-treated tumors (Fig. 5C) likely reflects increased apoptosis.

Interestingly, the 34-mer-treated prostate cancer xenografts also showed decreases in microvessel density and diameter as well as increased apoptosis; however, these changes were less dramatic than in P18-treated tumors (Fig. 5A and B).

P18* in vivo *targets correlate with PEDF angioinhibitory signaling. PEDF and the 34-mer block angiogenesis by inducing endothelial cell apoptosis. Key events leading to the PEDF-dependent apoptosis are the induction of intrinsic cell death pathway, where PEDF elicits the production of the CD95L, which binds to the VEGF/bFGF-stimulated CD95 on the activated endothelial cells and thus initiates caspase-8- and caspase-3-dependent apoptosis (27). On the other hand, PEDF activates membrane-bound γ-secretase and thus reduces the levels of the endothelial VEGFR (VEGFR1; ref. 20). To ascertain that P18 recapitulates the main events typical for PEDF antiangiogenic epitope, we analyzed the vasculature in P18-treated and control (bFGF) Matrigel plugs for expression of CD95, CD95L, and VEGFR. As expected of the endothelium activated with bFGF, the majority of the microvessels stained positive for CD95 in control plugs regardless of the presence of

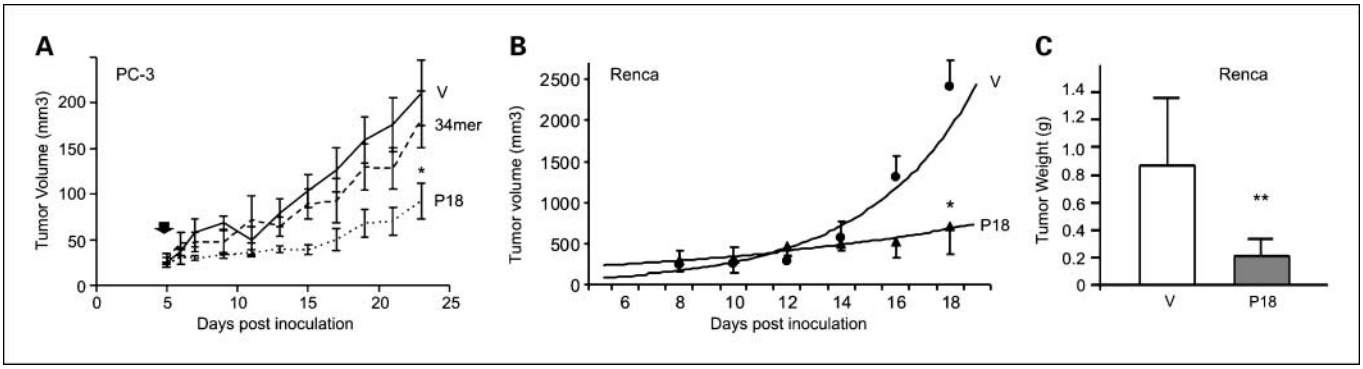

Fig. 4. Inhibition of tumor growth by P18. *A,* treatment of the xenografted human prostate cancer (PC-3 cells, flank model) with the 34-mer and P18. P18 or the 34-mer were given at 10 mg/kg every 2 d after the tumors became visible and palpable. Note significant delay in the growth of the P18-treated tumors (*, $P < 0.001$). Tumor volumes were calculated as $V = \text{length} \times \text{width}^2 \times 0.52$. Data from the two independent experiments (five animals per group) were pulled together and analyzed with repeated-measures ANOVA. *B,* treatment of the xenografted mouse RCC (Renca cells, flank model; 10 animals per group). The tumors were allowed to establish (100-200 mm^3). P18 was administered and the tumor volumes were calculated as in *A*. *, $P < 0.004$. *C,* tumors were excised and weighted at the endpoint of experiment. **, $P < 0.0002$.

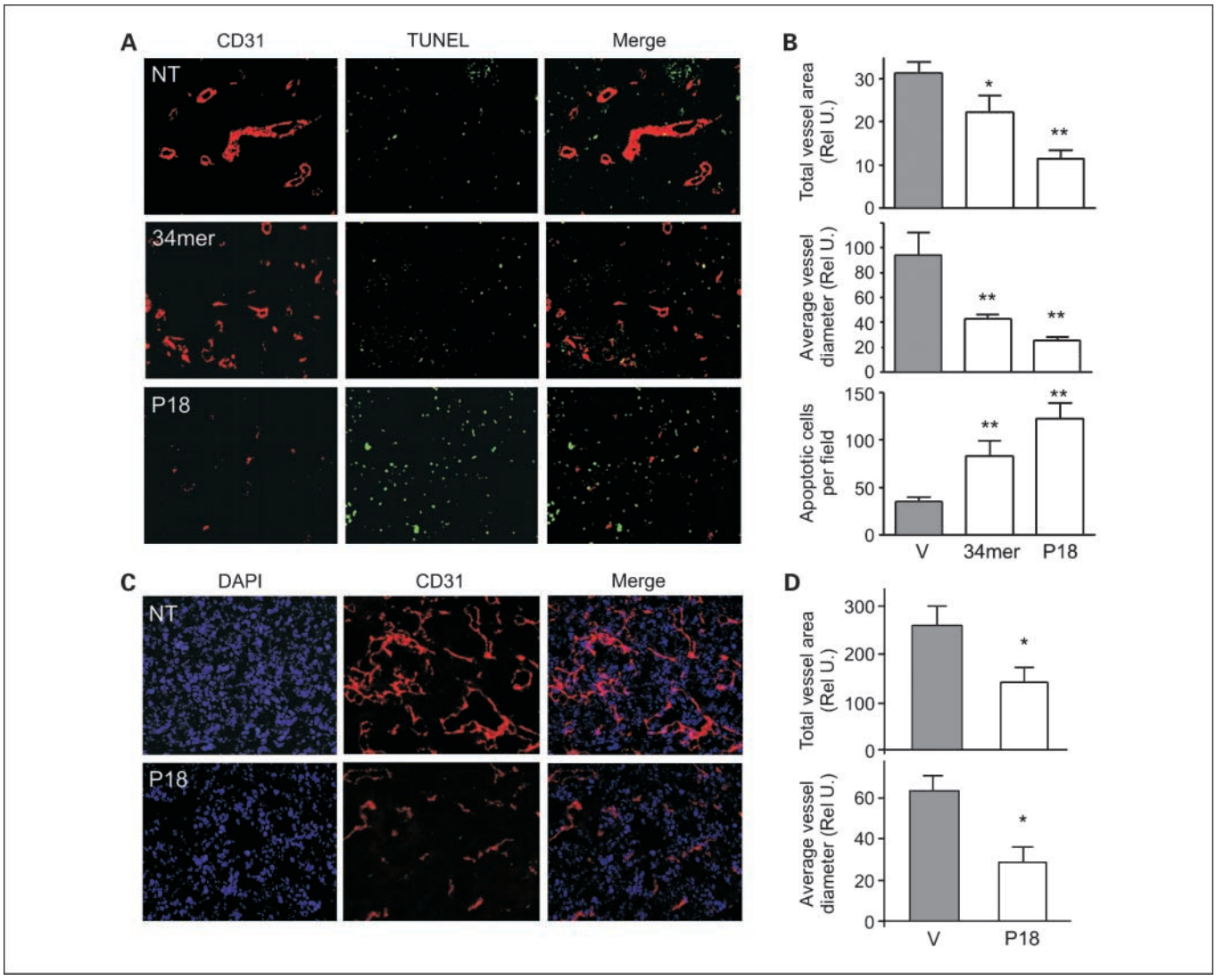

Fig. 5. Inhibition of tumor angiogenesis by P18. *A* and *B,* prostate tumor xenografts from the mice treated with 34-mer, P18 or vehicle control (*V*) were sectioned and stained for CD31 endothelial marker (*red*). Apoptosis was visualized by *in situ* TUNEL (*green*). Representative sections (*A*). *B,* total vascular area (*top*), average vessel diameter (*middle*), and number of apoptotic cells per ×10 field (*bottom*) were determined using MetaMorph software. *, $P < 0.01$; **, $P < 0.001$, statistically significant differences compared with bFGF (one-way ANOVA followed by Dunnett's multiple comparison test). *C* and *D,* Renca tumors treated with P18 or vehicle were sectioned and stained for CD31 to visualize microvasculature (*red*). The sections were counterstained with 4′,6-diamidino-2-phenylindole (DAPI, *blue*) to visualize nuclei. Representative sections (*C*). *D,* vascular area (*top*) and average vessel diameter (*bottom*) were determined as above. Note dramatic decrease in the vascularization and decreased cellularity of the P18-treated tumors.

the 34-mer or P18 (Fig. 6A). In contrast, CD95L was high in the vasculature treated with the 34-mer or P18 (60% and 83% positive microvessels, respectively) but not in the control plugs (32% positive vessels; $P < 0.001$; Fig. 6B). The differences between the 34-mer and P18 were also statistically significant ($P < 0.01$, Tukey's multiple comparison test). Finally, in control, 60% of the vessels were positive for VEGFR; 34-mer caused no significant reduction (51%), whereas in P18-treated plugs only 29% of the vessels were VEGFR positive ($P < 0.001$ and $P < 0.01$ versus control and 34-mer, respectively; Fig. 6C).

Discussion

In this study, we sought to identify minimal PEDF derivative, which retains antiangiogenic activity of the whole molecule. In our previous studies, we have mapped PEDF antiangiogenic activity to the 34-mer NH_2-terminal surface epitope. Here, we further narrowed down this region to 18 amino acids, the residues 39 to 57 on the PEDF molecule. The longer P23 peptide (residues 34-57) failed to block endothelial cell chemotaxis but induced apoptosis; shorter P14 (residues 41-57) blocked chemotaxis but had no effect on apoptosis. Neither P23 nor P14 showed antiangiogenic activity *in vivo*: moreover, P14 had stimulatory activity of its own. Of all the peptides, only P18 exhibited activity and specificity similar or superior to that of the parental 34-mer. P18 inhibited chemotaxis and induced apoptosis in the activated endothelial cells similar to the parental PEDF and the 34-mer. *In vivo*, P18 blocked bFGF- and VEGF-dependent angiogenesis in the cornea, in subcutaneous Matrigel plugs, and in DIVAA.

P18-specific activity was superior compared with the native PEDF and the 34-mer *in vitro* in the chemotaxis and apoptosis

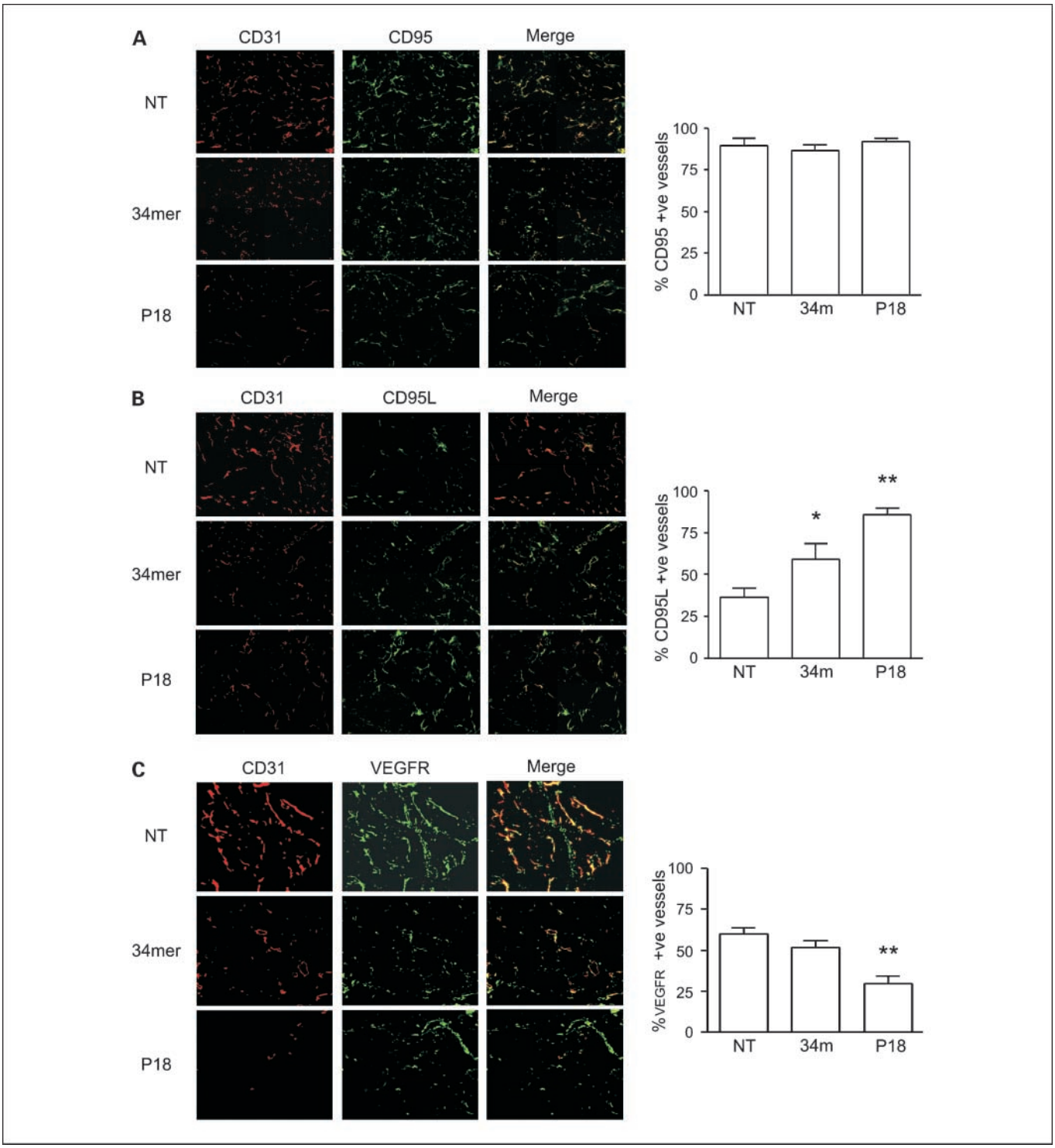

Fig. 6. P18 and PEDF share molecular targets on remodeling vasculature. Matrigel plugs containing bFGF (100 ng/mL) alone or in combination with the 34-mer or P18 were snap-frozen, sectioned, and stained for CD31 (*red*) to visualize the vasculature and for three critical PEDF vascular targets: CD95 (*A*), CD95L (*B*), and VEGFR (*C*). Total number of vascular structures and the number of microvessels positive for CD95, CD95L, and VEGFR, respectively, was quantified using MetaMorph software; the percent of the structures positive for each respective marker was calculated and compared between treatments. $P < 0.05$, statistically significant difference with control and other treatments (one-way ANOVA followed by Tukey's multiple comparison test).

assays (IC_{50} values for P18, 34-mer, and PEDF are 1 pmol/L, 10 pmol/L, and 1 nmol/L, respectively). *In vivo*, P18 was also more effective than the 34-mer: it was 10 times more potent at inducing apoptosis of the vascular endothelium and at reducing MVD in the Matrigel plugs and, more importantly, in prostate cancer model. It is possible that shorter P18 maintains conformational stability in solution better than the longer 34-mer peptide.

In our previous studies, we have shown that PEDF and the 34-mer block angiogenesis in the activated endothelium via the cascade, which causes accumulation of the message and increased expression of CD95L, a death ligand for the intrinsic death receptor (13, 27). This receptor, CD95, is in turn directed to the surface only in the inducer activated endothelial cells (27). Moreover, P18 shares another target with PEDF: earlier study showed that PEDF-dependent activation of γ-secretase leads to VEGFR cleavage and decreased angiogenesis (20). Thus, we generated short antiangiogenic peptide derivative that reproduced main signaling functional and signaling events that lead to cessation of angiogenesis by parental PEDF with high specific activity and, like PEDF, affects only remodeling endothelium.

Parental PEDF has been shown to affect growth and invasion of the nonendothelial cells: it induces apoptosis in cultured glioma, osteosarcoma, and prostate cancer cells and the anoikis of melanoma cells (28–30). Moreover, it suppresses invasion of the tumor cells, including melanoma and glioma (31, 32). However, PEDF effect on proliferation and invasion of the osteosarcoma cells was mediated by the more distal peptides, distinct from the 34-mer: residues 78 to 102 predominantly inhibited proliferation, whereas residues 90 to 114 increased adhesion to collagen type-1 and residues 387 to 411 were important for the inhibition of Matrigel invasion (33). Furthermore, amino acids 40 to 64 of the PEDF molecule cause osteogenic differentiation in osteosarcoma cells (33). This is consistent with the prodifferentiating activity of the 44-mer PEDF fragment (residues 58-101; refs. 13, 14). Thus, the direct effect of P18 on the tumor cells is less likely than its angiogenesis-mediated effects: we evaluated the action of P18 and of P34 on proliferation of the PC-3 cells and found no significant changes.

P18 inhibited the growth of androgen-independent prostate cancer and more aggressive RCC *in vivo* in the subcutaneous xenograft model at 10 mg/kg: at this dose, the 34-mer had no significant effect on tumor growth. In concert, P18 was more potent at blocking tumor angiogenesis and caused higher levels of intratumoral apoptosis. These findings also reflect superior potency of the P18 in comparison with the 34-mer.

In conclusion, we generated short peptide from PEDF antiangiogenic region, which retains only PEDF antiangiogenic function and is active in low picomolar range of concentrations. This peptide, P18, inhibits tumor growth and angiogenesis with high potency and is a novel, highly effective biotherapeutic agent for cancer treatment to be used alone or in combination with other agents.

Disclosure of Potential Conflicts of Interest

V. Shifrin, R. Beckmann, and C. Polsky are employed by Arbus Pharmaceutical, Inc.

References

1. Folkman J, Hanahan D. Switch to the angiogenic phenotype during tumorigenesis. Princess Takamatsu Symp 1991;22:339–47.
2. Desai AA, Stadler WM. Novel kinase inhibitors in renal cell carcinoma: progressive development of static agents. Curr Oncol Rep 2005;7:116–22.
3. Ferrara N, Hillan KJ, Gerber HP, Novotny W. Discovery and development of bevacizumab, an anti-VEGF antibody for treating cancer. Nat Rev Drug Discov 2004;3:391–400.
4. Mariani SM. Anti-angiogenesis: the challenges ahead. Med Gen Med 2003;5:22.
5. Sund M, et al. Function of endogenous inhibitors of angiogenesis as endothelium-specific tumor suppressors. Proc Natl Acad Sci U S A 2005;102:2934–9.
6. Bouck N, Stellmach V, Hsu SC. How tumors become angiogenic. Adv Cancer Res 1996;69:135–74.
7. Folkman J. Endogenous angiogenesis inhibitors. APMIS 2004;112:496–507.
8. Dawson DW, Volpert OV, Gillis P, et al. Pigment epithelium-derived factor: a potent inhibitor of angiogenesis. Science 1999;285:245–8.
9. Ek ET, Dass CR, Choong PF. PEDF: a potential molecular therapeutic target with multiple anti-cancer activities. Trends Mol Med 2006;12:497–502.
10. Fernandez-Garcia NI, Volpert OV, Jimenez B. Pigment epithelium-derived factor as a multifunctional antitumor factor. J Mol Med 2007;85:15–22.
11. Becerra SP. Focus on molecules: pigment epithelium-derived factor (PEDF). Exp Eye Res 2006;82:739–40.
12. Tombran-Tink J. The neuroprotective and angiogenesis inhibitory serpin, PEDF: new insights into phylogeny, function, and signaling. Front Biosci 2005;10:2131–49.
13. Filleur S, et al. Two functional epitopes of pigment epithelial-derived factor block angiogenesis and induce differentiation in prostate cancer. Cancer Res 2005;65:5144–52.
14. Becerra SP. Structure-function studies on PEDF. A noninhibitory serpin with neurotrophic activity. Adv Exp Med Biol 1997;425:223–37.
15. Smith ND, Schulze-Hoepfner FT, Veliceasa D, et al. Pigment epithelium-derived factor and interleukin-6 control prostate neuroendocrine differentiation via feed-forward mechanism. J Urol 2008;179:2427–34.
16. Notari L, et al. Identification of a lipase-linked cell membrane receptor for pigment epithelium-derived factor. J Biol Chem 2006;281:38022–37.
17. Apte RS, Barreiro RA, Duh E, Volpert O, Ferguson TA. Stimulation of neovascularization by the anti-angiogenic factor PEDF. Invest Ophthalmol Vis Sci 2004;45:4491–7.
18. Amorino GP, Parsons SJ. Neuroendocrine cells in prostate cancer. Crit Rev Eukaryot Gene Expr 2004;14:287–300.
19. Sulochana KN, Ge R. Developing antiangiogenic peptide drugs for angiogenesis-related diseases. Curr Pharm Des 2007;13:2074–86.
20. Cai J, Jiang WG, Grant MB, Boulton M. Pigment epithelium-derived factor inhibits angiogenesis via regulated intracellular proteolysis of vascular endothelial growth factor receptor 1. J Biol Chem 2006;281:3604–13.
21. Good DJ, Polverini PJ, Rastinejad F, et al. A tumor suppressor-dependent inhibitor of angiogenesis is immunologically and functionally indistinguishable from a fragment of thrombospondin. Proc Natl Acad Sci U S A 1990;87:6624–8.
22. Kenyon BM, Voest EE, Chen CC, Flynn E, Folkman J, D'Amato RJ. A model of angiogenesis in the mouse cornea. Invest Ophthalmol Vis Sci 1996;37:1625–32.
23. Passaniti A, et al. A simple, quantitative method for assessing angiogenesis and antiangiogenic agents using reconstituted basement membrane, heparin, and fibroblast growth factor. Lab Invest 1992;67:519–28.
24. Wang L, Schmitz V, Perez-Mediavilla A, Izal I, Prieto J, Qian C. Suppression of angiogenesis and tumor growth by adenoviral-mediated gene transfer of pigment epithelium-derived factor. Mol Ther 2003;8:72–9.
25. Polverini PJ, Bouck NP, Rastinejad F. Assay and purification of naturally occurring inhibitor of angiogenesis. Methods Enzymol 1991;198:440–50.
26. Zaichuk TA, Shroff EH, Emmanuel R, Filleur S, Nelius T, Volpert OV. Nuclear factor of activated T cells balances angiogenesis activation and inhibition. J Exp Med 2004;199:1513–22.
27. Volpert OV, Zaichuk T, Zhou W, et al. Inducer-stimulated Fas targets activated endothelium for destruction by anti-angiogenic thrombospondin-1 and pigment epithelium-derived factor. Nat Med 2002;8:349–57.
28. Ek ET, Dass CR, Contreras KG, Choong PF. Inhibition of orthotopic osteosarcoma growth and metastasis by multitargeted antitumor activities of pigment epithelium-derived factor. Clin Exp Metastasis 2007;24:93–106.
29. Doll JA, et al. Pigment epithelium-derived factor regulates the vasculature and mass of the prostate and pancreas. Nat Med 2003;9:774–80.
30. Garcia M, et al. Inhibition of xenografted human melanoma growth and prevention of metastasis development by dual antiangiogenic/antitumor activities of pigment epithelium-derived factor. Cancer Res 2004;64:5632–42.
31. Ek ET, Dass CR, Contreras KG, Choong PF. Pigment epithelium-derived factor overexpression inhibits orthotopic osteosarcoma growth, angiogenesis and metastasis. Cancer Gene Ther 2007;14:616–26.
32. Guan M, Pang CP, Yam HF, Cheung KF, Liu WW, Lu Y. Inhibition of glioma invasion by overexpression of pigment epithelium-derived factor. Cancer Gene Ther 2004;11:325–32.
33. Ek ET, Dass CR, Contreras KG, Choong PF. PEDF-derived synthetic peptides exhibit antitumor activity in an orthotopic model of human osteosarcoma. J Orthop Res 2007;25:1671–80.